NEUTRON STARS, PROTONEUTRON STARS, VACUUM CORRECTIONS AND GRAVITATIONAL WAVES IN NONLINEAR RELATIVISTIC QHD MODELS: AN OVERVIEW

C.A.Z. VASCONCELLOS

Instituto de Física, Universidade Federal do Rio Grande do Sul
91501-970 Porto Alegre, Rio Grande do Sul, Brazil
cesarzen@if.ufrgs.br

J. A. DE FREITAS PACHECO

Observatoire de la Côte d'Azur, Nice, France
pacheco@obs-nice.fr

In this work we review a few topics related to the determination of properties of neutron stars: the modeling of the equation of state of nuclear matter (EoS) at $T = 0$ and at finite T; the role of vacuum corrections in the EoS at high density and, finally, neutron stars as potential sources of gravitational waves. In the first part of this contribution, we consider a relativistic model for nuclear matter and neutron stars with a suitable parametrization of the nonlinear couplings involving mesons and baryons. For appropriate choices of the parameters, the model recovers current QHD models. We apply and test our framework on the description of static properties of neutron stars and we show that, for other sets of parameters, our approach gives consistent new physical results. In the second part, nuclear matter at finite T is studied in the framework of an effective many-body RFT and the Sommerfeld approximation, considering moreover the fundamental baryon octet and leptonic degrees of freedom, trapped neutrinos, chemical equilibrium and charge neutrality of the star. Our predictions include the determination of the mass of protoneutron stars, a description of structural aspects of the nuclear matter phase transition via an analysis of the behavior of the specific heat and, — through the inclusion of quark degrees of freedom —, of the properties of a hadron-quark phase transition in hybrid stars. In the third part, on the basis of the modified relativistic Hartree approximation, applied to the Walecka σ-ω model, and the relativistic Hartree approximation, employed in the nonlinear Boguta-Bodmer model, the role of vacuum corrections in nuclear matter is investigated. Mathematical constraints between the parameters of these formulations show that, after including hyperon and lepton degrees of freedom, electric charge neutrality and chemical equilibrium, their predictions for global static properties of neutron star matter exhibit expressive differences. In the forth part of this contribution we review, on basis of the planned sensitivity of present laser interferometers (VIRGO or LIGO I) and those of the next generation (LIGO II), the potential detectability of gravitational waves generated by oscillations excited during a phase transition from hadronic matter to deconfined quark-gluon matter in the core of a neutron star considering respectively a Boguta-Bodmer based model and the MIT bag model. We conclude that the maximum distance probed by the detectors of the first generation is well beyond M31, whereas the second generation detectors will probably see phase transition implications at distances two times larger, but certainly not yet attaining the Virgo cluster.

Introduction

In the last few decades, studies on the internal structure, composition, dynamics and evolution of protoneutron stars, neutron stars, pulsars, hybrid and strange stars became central topics for theoretical and experimental research. The first pulsar was observed[1] in 1967 and characteristic observational features allowed its identification as a rotating neutron star. Since then, nuclear models have been more widely employed, than the past, in the description of the *holly graal of modern physics*, the equation of state (EoS) of dense matter. As under the pull of gravity the energy density in the core of these compact stars is thought to strongly exceed the density of ordinary nuclear matter, predictions on the structure of the stars depend sensitively on the EoS provided by model calculations. Combined with the equations of the general relativistic metric, predictions on the mass, radius, crust extent and moment of inertia of the stars are then susceptible to the comparison to observation[2]. The models should also provide the description of other relevant dynamical properties of these compact stars as the rotational period, the emission of neutrinos and gravitational waves and the phase transition of hadron matter to a quark-gluon plasma. Presently, the best mass determination of neutron stars corresponds to the binary pulsar PSR 1913+16, for which the mass is $M = 1.444 M_{\odot}$. Other estimates based on quasi-periodic oscillations, observed in the X-ray emission of low mass binaries suggest values up to $2.0 - 2.2 M_{\odot}$; these results are however quite uncertain due to the modelling dependence on the data analysis. More recently, from new radial velocity data, the mass of the neutron star associated to the X-ray source in the system Vela X-1 was recalculated[3] with a larger accuracy than preceding estimates: the resulting value is $1.86 \pm 0.16 M_{\odot}$. For a given family of stars, a stiffer EoS predicts higher limiting mass and larger radii ($R > 10 - 12$ km).

From the theoretical point of view, quantum chromodynamics (QCD) should in principle provide the most profound delineation of the complex baryonic composition of neutron stars. However, as is well known, the strongly nonlinear behavior of QCD at the hadronic energy scales inhibits any practical calculation. This limitation has lead theorists to search for phenomenological effective descriptions of the structure of nuclear matter at the high density domain as, for instance, the approach developed by J.D. Walecka[4], quantum hadrodynamics (QHD). QHD is a relativistic quantum field theory based on a local lagrangian density with the nucleon and the scalar-isoscalar, attractive, σ-meson and the vector-isoscalar, repulsive, ω-meson as the relevant effective mean-field degrees of freedom. This model provides a consistent theoretical framework for the description of bulk static properties of strong interacting

many-body nuclear systems under the extreme conditions of pressure and density as the ones found in neutron stars. An alternative approach, the nonlinear model of J. Boguta and A.R. Bodmer[5] was developed to improve the description of some of the static properties of nuclear matter, more precisely, the nucleon effective mass, M^*, and the compression modulus of symmetric nuclear matter, K. With cubic and quartic self-interaction scalar terms, the model has two additional parameters which allow and provide sufficient flexibility to reproduce, at saturation density, currently accepted values for the compression modulus of symmetric nuclear matter and the nucleon effective mass[6,7,8].

In the following we review a few topics related to the determination of properties of neutron stars: the modelling of the equation of state of nuclear matter (EoS) at $T = 0$ and at finite temperature, in sections 1 and 2; the role of vacuum corrections in the EoS at high density, in section 3, and, finally, in section 4, neutron stars as potential sources of gravitational waves.

1 A Parameterized Class of Nonlinear Relativistic Models

We proposed recently[6,7] a phenomenological lagrangian with nonlinear meson-baryon couplings[a]:

$$\mathcal{L} = \mathcal{L}_{free} + \sum_B \bar{\psi}_B \left(g^\star_{\lambda\sigma B}\sigma - g^\star_{\beta\omega B}\gamma_\mu\omega^\mu - \frac{1}{2} g^\star_{\gamma\varrho B}\gamma_\mu \boldsymbol{\tau}\cdot\boldsymbol{\varrho}^\mu \right) \psi_B \,. \qquad (1)$$

This lagrangian density describes a system of eight baryons ($B = p$, n, Λ, Σ^-, Σ^0, Σ^+, Ξ^-, Ξ^0) coupled to three mesons (σ, ω, ϱ) and two leptons (e, μ) (in the present case we have assumed $b = c = 0$; for the details see Ref.[7]) with new coupling constants:

$$g^\star_{\sigma\lambda B} \equiv m^\star_{\lambda B} g_\sigma \;;\; g^\star_{\omega\beta B} \equiv m^\star_{\beta B} g_\omega \;;\; g^\star_{\varrho\gamma B} = m^\star_{\gamma B} g_\varrho \,;$$
$$m^\star_{nB} \equiv (1 + \frac{g_\sigma \sigma}{n M_B})^{-n} \,;\; n = \lambda, \beta, \gamma \,. \qquad (2)$$

[a] W. Koepf *et al.*[9] have studied the contribution of the scalar term $\mathcal{L}_{\sigma N} = M\bar{m}^\star(\sigma)\bar{\psi}\psi$ in the strong interacting lagrangian density. N.K. Glendenning *et al.*[10] have analyzed a coupling term of the type $\bar{m}^\star = (1 - (g_\sigma\sigma/2M))(1 + (g_\sigma\sigma/2M))^{-1}$, obtaining, at saturation density, for the nucleon effective mass, $M^*/M = 0.796$ and for the compression modulus of nuclear matter, $K = 265 MeV$. From the relation $M^*/M \sim 1 - (g_\sigma\sigma/M)$, the experimental results suggest, at nuclear saturation density, $M^*/M \sim 0.70$, giving $g_\sigma\sigma/M \sim 0.3$. Thus, these different models just add scalar self-coupling correction terms to the minimum coupling expression of the Walecka model.

(a)

Model	λ	β	γ
Walecka	0	0	0
ZM	1	0	0
ZM3	1	1	1

(b)

$\bar{m}^\star(\sigma)$	M^*/M	$K(MeV)$
$1-\frac{g_\sigma\sigma}{M}$	0.55	545
$1-tanh(\frac{g_\sigma}{M}\sigma)$	0.71	410
$exp(-\frac{g_\sigma\sigma}{M})$	0.80	265
$(1+\frac{g_\sigma\sigma}{M})^{-1}$	0.85	233

Table 1. On the left ((a)) we show values of λ, β and γ for different QHD models (ZM and ZM3 refer to the models of J. Zimanyi, S.A. Moszkowski[11]). On the right ((b)), values of the nucleon effective mass and compression modulus of symmetric nuclear matter, at saturation density, for different types of couplings between the scalar mesons and the nucleon fields (see Ref.[9]) are shown.

We assume λ, β and γ as real and positive numbers (the range of best phenomenology). Thus, this approach corresponds to a rescaling of standard scalar, vector and isovector coupling terms; for instance,

$$g_\sigma\sigma\bar{\psi}\psi \rightarrow g^\star_\sigma\bar{\psi}\sigma\psi = \frac{g_\sigma\sigma}{\left(1+\frac{g_\sigma\sigma}{\lambda M}\right)^\lambda}\bar{\psi}\psi\,. \tag{3}$$

Similar interaction terms may be associated to the vector and isovector sectors of the lagrangian density. Table 1 exhibits on the left the correspondence between this and other current models and on the right values for the nucleon effective mass (M^*) and compression modulus of symmetric nuclear matter (K) for different types of scalar meson-baryon couplings. From the eigenvalues of the Dirac equation, the baryon Fermi energy is: $\mu_B(k) = g^\star_{\omega B}\omega_0 + g^\star_{\varrho B}\varrho_{03}I_{3B} + \sqrt{k^2_{F,B}+(M_B-g^\star_{\sigma B}\sigma)^2}$. For instance, the corresponding expressions for the scalar and vector potentials are, respectively, $S = -m^*_\lambda g_\sigma\sigma$ and $V = m^*_\beta g_\omega\omega_0$. We see from these results combined with the definitions of the effective coupling constants that this model allows the controlling on the intensity of the scalar, vector and isovector mean-field potentials. Variations of the parameters permit to obtain values of S, V, M^* and K which correspond to the intermediate regions of values of Walecka, ZM3 and ZM models. Indeed, the range of possible values for the parameters of the theory is not very large. Due to the form of the new couplings, there occurs a rapid convergence to exponential forms: for λ and/or $\beta = \gamma > 2$ the results of this model do not strongly differ from the results of the model with exponential couplings

$$g^\star_{\sigma\lambda B} \overset{\lambda\rightarrow\infty}{\longrightarrow} e^{-\frac{g_\sigma\sigma}{M_B}}g_\sigma\ ;\ \ g^\star_{\omega\beta B} \overset{\beta\rightarrow\infty}{\longrightarrow} e^{-\frac{g_\sigma\sigma}{M_B}}g_\omega\ ;\ \ g^\star_{\varrho\gamma B} \overset{\gamma\rightarrow\infty}{\longrightarrow} e^{-\frac{g_\sigma\sigma}{M_B}}g_\varrho\,. \tag{4}$$

In the following, we consider two cases: case S (scalar), with variations of λ keeping $\beta = \gamma = 0$; it contains the results of the Walecka and ZM models (see table 3); case S-V (scalar-vector), with variations of λ, keeping $\beta = \gamma = \lambda$;

Model	$(\frac{g_\sigma}{m_\sigma})^2$	$(\frac{g_\omega}{m_\omega})^2$	$(\frac{g_\rho}{m_\rho})^2$	$M^\star/M$	K	S	V
ZM	7.94	2.84	5.23	0.85	224	-140	84
ZM3	19.57	13.45	9.06	0.71	159	-267	204

Table 2. Values of coupling constants, nucleon effective mass, compression modulus of nuclear matter and scalar and vector potentials at saturation density (ZM and ZM3 models) (see Ref.[6,7]). $((\frac{g_i}{m_i})^2$ are given in fm^2 and K, S, and V in MeV.)

λ	$log(\varepsilon_c)$ g/cm^3	$M_\star$ $(M_\odot)$	$R_\star$ (km)	S (MeV)	z	$\frac{Y}{A}$	N_{BT} $(\times 10^{58})$	K (MeV)	$\frac{M^\star}{M}$	R
0	15.18	2.77	13.17	936	0.623	0.27	0.40	566	0.537	0.931
0.07	15.38	2.17	10.89	923	0.554	0.34	0.30	258	0.694	0.957
0.15	15.52	1.77	9.59	857	0.479	0.35	0.24	216	0.779	0.965
0.30	15.52	1.59	9.61	669	0.399	0.27	0.21	214	0.822	0.969
0.60	15.49	1.58	9.86	480	0.377	0.22	0.21	223	0.843	0.970
1.00	15.47	1.59	9.98	401	0.372	0.20	0.21	224	0.850	0.970
1.50	15.47	1.59	9.98	366	0.373	0.20	0.21	226	0.854	0.971
∞	15.47	1.59	10.00	350	0.373	0.20	0.21	228	0.856	0.971

Table 3. Stellar properties for the S case: ε_c - central density;$M_\star$ - star mass; $R_\star$ - star radius; S - scalar potential in the star center; z - redshift; Y/A is the hyperon/baryon ratio and N_{BT} is the total baryonic number. All this quantities are evaluated for the neutron star with the maximum mass in the sequence. Moreover we show values for the compression modulus K and the nucleon effective mass $M^\star/M$ at saturation density and the relativistic coefficient R (see Ref.[6,7]).

Walecka and ZM3 models belong to this category (see table 4). (Walecka model belongs to both categories because in this model the λ, β and γ parameters are null.)

In the determination of the EoS for neutron stars, we take into account chemical equilibrium, baryon number and electric charge conservation. Combining the resulting EoS with the Tolman-Oppenheimer-Volkoff (TOV) equations[12,13] we obtain values for static properties of neutron stars. Typical results in our approach can be found in Figs. 1 and 2. In particular, the ZM model predicts a maximum mass of approximately $1.6M_\odot$. The ZM3 model is very soft and predicts a very small maximum neutron star mass, $\sim 0.72M_\odot$. It may be surprising, at a first glance, that the maximum neutron star mass for the Walecka model with hyperons ($2.77M_\odot$) exceeds the well known result ($2.6M_\odot$) found in Ref.[4] for stars just composed of neutrons, since the addition of hyperons produces the softening of the EoS, lowering the resulting star mass. This apparent contradiction can be explained by the extreme sensibility

λ	$log(\varepsilon_c)$	$M_\star$	$R_\star$	S	z	$\frac{Y}{A}$	N_{BT}	K	$\frac{M^\star}{M}$	R
	g/cm^3	$(M_\odot)$	(km)	(MeV)			$(\times 10^{58})$	(MeV)		
0	15.18	2.77	13.17	936	0.623	0.27	0.40	566	0.537	0.931
0.07	15.24	2.56	12.39	960	0.602	0.30	0.37	417	0.561	0.936
0.15	15.33	2.30	11.38	985	0.574	0.34	0.32	311	0.587	0.941
0.30	15.51	1.83	9.58	1011	0.516	0.39	0.25	218	0.630	0.949
0.60	15.62	1.07	8.08	891	0.282	0.35	0.14	169	0.682	0.955
1.00	15.31	0.72	9.76	577	0.128	0.10	0.09	159	0.710	0.959
1.50	15.18	0.67	10.21	468	0.113	0.04	0.08	156	0.728	0.961
∞	15.14	0.66	10.31	431	0.110	0.03	0.08	155	0.738	0.961

Table 4. Stellar properties for the S-V case. Same correspondences as in table 3.

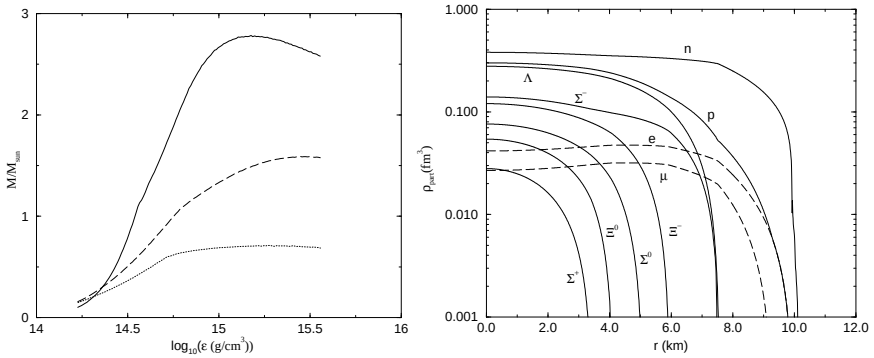

Figure 1. *On the left, neutron star mass as a function of the central density in Walecka (solid line), ZM (dashed line) and ZM3 (dotted line) models. On the right, radial distribution of the different leptonic and baryonic species in the ZM model.*

of this kind of theory on the specific choice of the values of the binding energy and saturation density. With our choice for these quantities, which is widely used in the recent literature, we get for the mass of a star composed only by neutrons the value of $3.05 M_\odot$, that is, a difference of almost a half solar mass! Using $a_4 = 33.6\, MeV$, we obtain $2.33 M_\odot$ for the mass of a neutron star with the inclusion of hyperons and leptons. In this way, extrapolation for neutron star densities from the fitting of B and ρ_0 at saturation needs more precision on the choice of these quantities. Our results indicate the same saturation of the electron chemical potential at $\sim 200\, MeV$ for the ZM and Boguta-Bodmer models with universal coupling. ZM3 model predicts, in the comparison to the other models, higher values for the mean-field expectation value of the ϱ meson potential, $-g_\varrho \varrho_{03}$, due to the large value for the ratio g_ϱ / m_ϱ in this

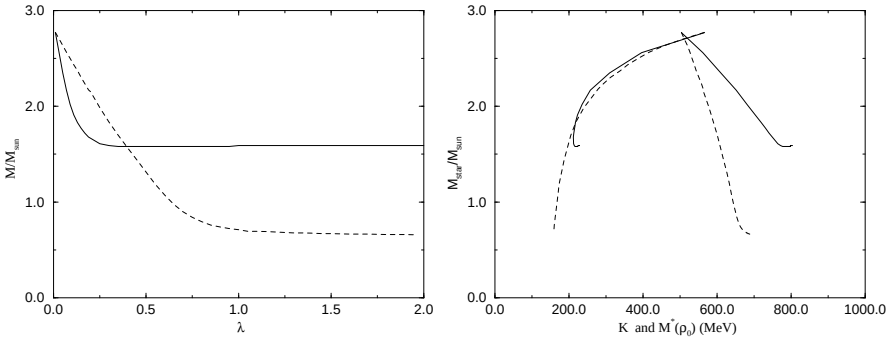

Figure 2. *On the left panel: maximum mass of a neutron star sequence (universal coupling) as a function of the λ parameter, for cases S (full line) and S-V (long dashed line). On the right panel: dependence of the maximum neutron star mass of a sequence with the compression modulus (left) and nucleon nonlinear mass at saturation (right). Solid line corresponds to the S case and dashed line to the $S-V$ case.*

model. The known problem of negative effective mass manifests itself dramatically in our results for the Walecka model. The nucleon effective mass is a dynamical quantity that expresses the screening of the baryon masses by the scalar meson condensate. As we add more and more baryonic species we open the possibility for the scalar potential $|S|$ to become larger than the free baryon masses M_B (see Ref.[6,7]):

$$M_B^\star = \left(M_B - \sum_{B' \neq B} \frac{g_\sigma^2}{m_\sigma^2} \frac{M_{B'}^\star}{\pi^2} \int \frac{k^2 dk}{\sqrt{k^2 + {M_{B'}^\star}^2}} \right) \Big/ \left(1 + \left(\frac{g_\sigma}{m_\sigma} \right)^2 \frac{1}{\pi^2} \int \frac{k^2 dk}{\sqrt{k^2 + {M_B^\star}^2}} \right) . \quad (5)$$

We cannot interpret the vanishing of the effective baryon mass as a signal of a phase transition to a quark-gluon plasma because our lagrangian model does not contain these underlying degrees of freedom. Additionally, at such high densities and strong meson fields we have already reached the critical density where the production of virtual baryon-antibaryon pairs is favored. In fact, this behavior of the effective baryon mass may indicate that the mean field approximation is being pushed to its limits of applicability. Finally, our results indicate that Walecka's baryonic distribution stabilizes after $\rho \sim 1.0 fm^{-3}$ and all species appear up till $\rho \sim 0.7 fm^{-3}$ which is approximately the density for which $|S|$ exceeds M_B. The lepton populations never vanish in the ZM distribution and even at $\rho \sim 1.2 fm^{-3}$ baryonic species are still emerging. Essentially, these differences are due to the strength of the scalar potential in

these two models, since a particle is created only when the condition

$$q_B\mu_n - q_{e,B}\mu_e \geq g^\star_{\omega B}\omega_0 + g^\star_{\rho B}\varrho_{03}I_{3B} + (M_B - g^\star_{\sigma B}\sigma)$$

is satisfied.

Having considered nuclear matter at $T = 0$ in the following we review a recently developed treatment for nuclear matter at finite T and apply our modeling in the study of the protoneutron star.

2 Finite Temperature Effective Field Theory for Protoneutron Stars

In the investigation of properties of nuclear matter at finite T, we consider a model containing the fundamental baryon octet, lepton degrees of freedom and trapped neutrinos, σ-, ω- and ϱ-meson fields, chemical equilibrium and charge neutrality[14,15]. Moreover, we exceed the limit of hadron degrees of freedom by including quarks in order to study the phase transition to quark matter[14,15]. We focus on a particular process in the evolution of compact stars preceding the supernova explosion: the formation of a hot and dense collapsed core or a *protoneutron star*[16], which can reach temperatures as high as few tens of MeV and which are formed in a type-II supernova explosion, which then evolves to a cold neutron star, basically through neutrino emission. Because of its very dense and hot core, the star is able to trap neutrinos, imparting momentum to the outer layers and then cooling as it reaches a quasi-equilibrium state. The evolution of protoneutron stars is studied using the Sommerfeld approximation. Global static properties as masses and radii are then computed as functions of central density and temperature[15].

The lagrangian density of our approach in the hadron sector is based on equation (1) with $b, c \neq 0$. The scalar and vector coupling constants in the theory, g_σ and g_ω, and the coefficients b and c for the nonlinear σ self-couplings are determined to reproduce, at saturation density, $\rho_0 = 0.153fm^{-3}$, the binding energy, $B = -16.3MeV$, the compression modulus, $K = 240MeV$, of symmetric nuclear matter, and the nucleon effective mass, $M^\star = 732MeV$. Additionally, the isovector coupling constant g_ϱ is determined from the asymmetry energy coefficient, $a_4 = 32.5MeV$, in nuclear matter. The hyperon/nucleon coupling constant ratios $\chi_i = g_{Hi}/g_i$, with $i = \sigma, \omega$, are constrained through the binding energy of the Λ-hyperon in nuclear matter, from hypernuclear spectroscopy and the lower bound of the mass of a neutron star. Neutrinos are included in our formulation, at chemical equilibrium, via the lepton fraction ratio $Y_L = (\rho_e + \rho_\nu)/\rho_B$, where ρ_e, ρ_ν and ρ_B represent, respectively, the

electron, neutrino and baryon densities. We extract the lepton fraction Y_L from the study of the gravitational collapse of the core of these stars.

Figure 3. On the left panel: protoneutron star maximum mass as a function of temperature for $Y_l = 0.4$ (solid line) and $Y_L = 0$ (dotted line). On the right panel: specific heat as a function of baryon density for T=10MeV.

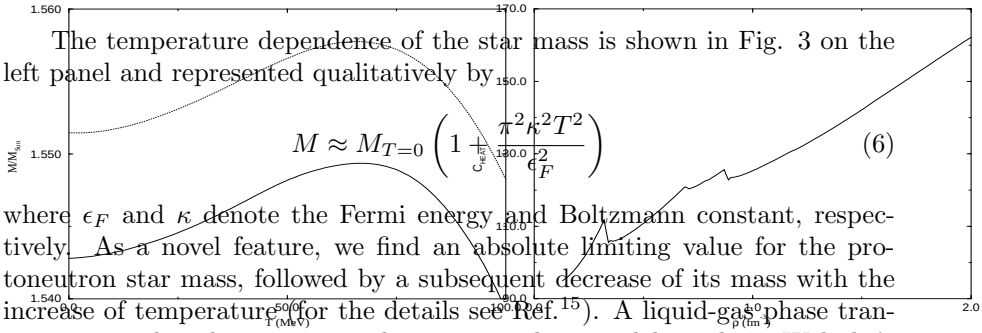

The temperature dependence of the star mass is shown in Fig. 3 on the left panel and represented qualitatively by

$$M \approx M_{T=0}\left(1 + \frac{\pi^2 \kappa^2 T^2}{\epsilon_F^2}\right) \tag{6}$$

where ϵ_F and κ denote the Fermi energy and Boltzmann constant, respectively. As a novel feature, we find an absolute limiting value for the protoneutron star mass, followed by a subsequent decrease of its mass with the increase of temperature (for the details see Ref.[15]). A liquid-gas phase transition is predicted in various relativistic nuclear models such as Walecka's QHD-I, Boguta-Bodmer and others when symmetric nuclear matter or pure neutron matter are considered. However, for asymmetric nuclear matter with the inclusion of the ϱ meson, this phase transition disappears. In this case, the energy used to generate the liquid-gas phase transition is now used in hyperon production processes, resulting in a phase transition of asymmetric nuclear matter into hyperon matter. As a signal of this phase transition, discontinuities on the specific heat can be found as a function of temperature. This phase transition is similar to the corresponding one which appears in the super-conductivity phenomena of electronic systems with the formation of Cooper pairs, where discontinuities are also found instead of singularities, as in a Van der Waals liquid-gas phase transition, characterizing the former as a continuous phase transition as shown in Fig. 3, on the right panel.

Additionally, in order to describe the quark matter EoS and the hadron-quark phase transition, we make use of the MIT bag model[17]. (for more details see Ref.[15]); the phase transition is determined via the Gibbs criteria[18] which require that, at constant temperature, pressure and chemical potential of both, hadron and quark phases are related for a given conserved overall baryon number. In Fig.4 on the left panel, the plateau reflects the Gibbs condition of the phase transition. The inclusion of quarks has a significant impact on the maximum mass of a neutron star; hybrid stars may develop a QGP core, which may extend several kilometers lowering its maximum mass due to the stiffening of the EoS. At even higher central densities we can find other classes of stars, for instance strange and quark stars, which are basically formed by deconfined quark matter with a thin (1 km) crust of nuclear matter. Finally, the results of Fig. 4, on the right panel, show that the Sommerfeld approximation is sufficient.

As the next topic of our study, we consider the role of self-couplings of the σ scalar meson in a QHD effective modelling of nuclear matter and neutron star matter.

Figure 4. On the left panel: equation of state for the hadron-quark phase transition for a bag constant $B = 100 MeV/fm^3$(solid line), $B = 131.2 MeV/fm^3$ (dotted line) and $B = 150 MeV/fm^3$ (dashed line). On the right panel: EoS corresponding to the Walecka model for T = 50 MeV and 10 MeV (upper and lower curves, respectively). Solid lines: exact results; dashed and dotted lines: first and second order corrections of the Sommerfeld approximation.

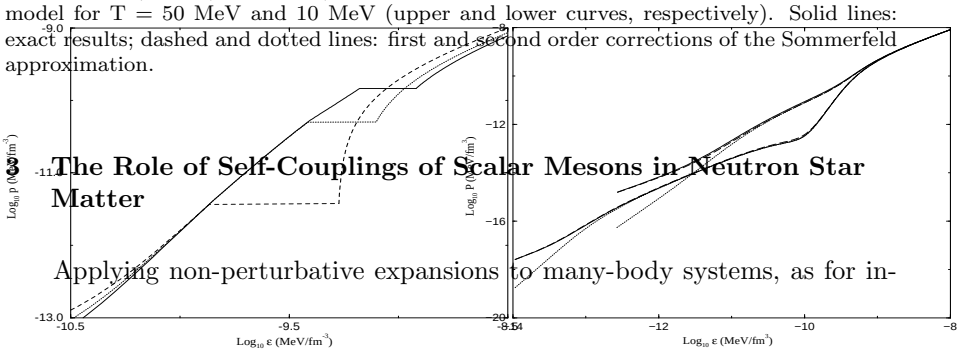

3 The Role of Self-Couplings of Scalar Mesons in Neutron Star Matter

Applying non-perturbative expansions to many-body systems, as for in-

stance the relativistic Hartree approximation[19], the simplest contributions to the baryon propagator are second-order tadpole diagrams. Feynman rules allow to express the second-order corrections to the baryon propagator in terms of second-order self-energy terms associated to scalar and vector meson fields. Self-consistency may be achieved by making use of interacting baryon and meson propagators in the nuclear medium to determine the scalar and vector self-energies. Dyson equation for the baryon propagator can be formally solved and the resulting expression is the sum of two terms: a divergent contribution which involves the propagation of virtual positive- and negative-energy quasi-nucleons, and a term which allows for quasi-nucleon holes inside the Fermi sea, which represents a correction to the former for the Pauli exclusion principle. Divergences then arise from a sum over all occupied states in the negative-energy sea of quasi-baryons. Walecka's mean field results for the energy density can then be achieved by dropping all divergent contributions from anti-baryons in the full interacting baryon propagator which renders the integrals for the scalar and vector self-energies finite. To have a hint on the role of vacuum corrections in neutron star matter, In the following we consider the relativistic Hartree approximation (RHA), applied to the Boguta-Bodmer model and the modified relativistic Hartree approximation applied to the Walecka model.

In the RHA, the divergent integrals over the occupied negative-energy states may be rendered finite by including appropriate scalar counterterms in the lagrangian density

$$\mathcal{L} = a_1\sigma + \frac{1}{2!}a_2\sigma^2 + \frac{1}{3!}\sigma^3 + \frac{1}{4!}\sigma^4 \tag{7}$$

(in this approach, only the scalar sector gives divergent contributions) and by defining a convenient set of renormalization conditions. Thus, in the RHA applied to the Walecka model, the resulting energy density $\mathcal{E}^{[W]}_{RHA}$ is the sum of the mean-field contribution, $\mathcal{E}^{[W]}_{MFA}$, and the one-loop vacuum correction, $\Delta\mathcal{E}^{[W]}_{RHA}$, caused by a shift in the single-particle nucleon spectra due to scalar meson self-interactions: $\mathcal{E}^{[W]}_{RHA} = \mathcal{E}^{[W]}_{MFA} + \Delta\mathcal{E}^{[W]}_{RHA}$, with

$$\begin{aligned}\Delta\mathcal{E}^{[W]}_{RHA} &= -\gamma\int_{Dirac\,Sea}\frac{d^3k}{(2\pi)^3}\sqrt{k^2+M^{\star 2}} \\ &= -\frac{1}{4\pi^2}\left[M^{*\,4}\ln\frac{M^*}{M} + M^3\,(g_\sigma\sigma) - \frac{7}{2}M^2\,(g_\sigma\sigma)^2 + \frac{13}{3}M\,(g_\sigma\sigma)^3 - \frac{25}{12}\,(g_\sigma\sigma)^4\right].\end{aligned} \tag{8}$$

Applying the RHA to the Boguta-Bodmer model it follows: $\mathcal{E}^{[BB]}_{RHA} =$

$\frac{\mu}{M}$	$(\frac{g_\sigma}{m_\sigma})^2$	$(\frac{g_\omega}{m_\omega})^2$	$(\frac{g_\varrho}{m_\varrho})^2$	$K(MeV)$	$\frac{M^*}{M}$
0.50	10.098	2.131	5.314	135.13	0.874
0.70	11.563	4.921	4.945	153.59	0.781
0.90	11.805	8.090	4.418	578.97	0.674
1.00	10.019	6.464	4.706	457.25	0.729
1.10	9.025	5.073	4.923	350.60	0.776
1.30	8.193	3.326	5.165	239.24	0.834

Table 5. Coupling constants, compression modulus of symmetric nuclear matter (K) and effective nucleon mass ratio (M^*/M), at saturation density, from the Walecka-MRHA model for different ratios μ/M.

$\frac{\mu}{M}$	$(\frac{g_\sigma}{m_\sigma})^2$	$(\frac{g_\omega}{m_\omega})^2$	$(\frac{g_\varrho}{m_\varrho})^2$	$b\times 100$	$c\times 100$	$K(MeV)$	$\frac{M^*}{M}$
0.50	10.117	2.131	5.314	5.8942	-7.1348	135.13	0.874
0.70	11.557	4.921	4.945	1.7229	-3.6160	153.59	0.781
0.90	11.794	8.090	4.418	0.1626	-1.0692	578.97	0.674
1.00	10.015	6.464	4.706	0.0010	-0.0045	457.25	0.729
1.10	9.024	5.073	4.923	0.1456	0.9551	350.60	0.776
1.30	8.198	3.326	5.165	1.1540	2.6188	239.24	0.834

Table 6. Coupling constants, compression modulus of nuclear matter (K) and the effective nucleon mass ratio (M^*/M) from the Boguta-Bodmer-RHA model for different ratios μ/M.

$\mathcal{E}^{[W]}_{MFA} + U(\sigma) + \Delta\mathcal{E}^{[W]}_{RHA} + \Delta\mathcal{E}^{[BB]}_{RHA}$. In this expression

$$\Delta\mathcal{E}^{[BB]}_{RHA} = \frac{m_\sigma^4}{(8\pi)^2}\left[(1+\phi_{12})^2\log(1+\phi_{12}) - \phi_{12} - \frac{3}{2}\phi_{12}^2 - \frac{1}{3}\phi_1^2(\phi_1+3\phi_2) + \frac{1}{12}\phi_1^4\right] \quad (9)$$

which denotes the RHA vacuum corrections due to the scalar meson self-coupling terms; in this expression: $\phi_{12} \equiv \phi_1 + \phi_2$; $\phi_1 = (2bM^2 g_\sigma^2\chi)/m_\sigma^2$; $\phi_2 = (3cM^2 g_\sigma^2\chi^2)/m_\sigma^2$; $\chi = g_\sigma\sigma/M$; $U(\sigma) = \frac{1}{3!}bM(g_\sigma\sigma)^3 + \frac{1}{4!}c(g_\sigma\sigma)^4$.

The renormalization procedure outlined before requires implicitly an arbitrary scale, μ. Using the *on-shell* renormalization scheme, with the choice $\mu = M$, one is left with the results[19] obtained by S.A. Chin. In the *minimal subtraction* renormalization scheme, μ can be optimized as a free parameter, leading to the MRHA[20,21]. In this approach the energy density for the Walecka model becomes $\mathcal{E}^{[W]}_{MRHA} = \mathcal{E}^{[W]}_{MFA} + \Delta\mathcal{E}^{[W]}_{RHA} + \Delta\mathcal{E}^{[W]}_{MRHA}$ with

$$\Delta\mathcal{E}^{[W]}_{MRHA} = \frac{M}{\pi^2}\left(1 - \frac{\mu}{M} + ln\frac{\mu}{M}\right)(g_\sigma\sigma)^3 + \frac{1}{4\pi^2}ln\frac{\mu}{M}(g_\sigma\sigma)^4 . \quad (10)$$

Our motivation is to find analytical relations between the b and c parameters of the Boguta-Bodmer-RHA and the Walecka-MRHA models for vacuum corrections in nuclear matter. Equating the expressions for the energy density

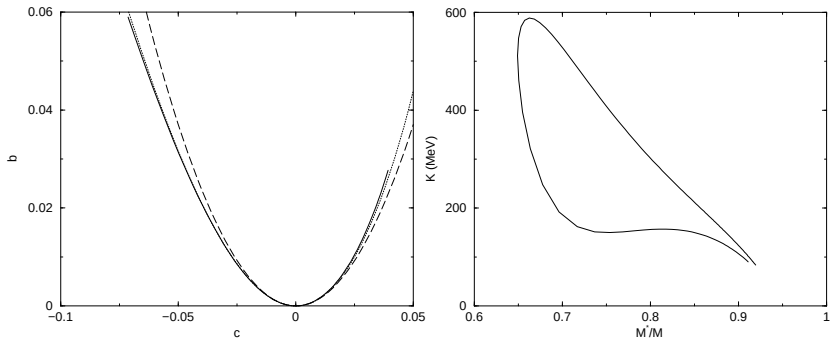

Figure 5. *On the left panel: the relation between the parameters b and c. On the right panel: compression modulus (K) of symmetric nuclear matter as a function of effective mass (M^*/M). Solid line refers to points in table (6); dotted line refers to the left relation on (11); dashed line refers to the parabolic relation on (11).*

at saturation density, we have found[8], for a given value of μ

$$b = -\frac{3}{\pi^2}(1 - e^{\pi^2 c} + \pi^2 c) \quad \text{or, since } c << 1, \text{ we have } \quad b \sim \frac{3\pi^2}{2} c^2 \,. \qquad (11)$$

Some of our results can be found in tables 5 and 6. Our study indicates that these two approaches render similar expressions for the EoS of nuclear matter up to the fifth order in the scalar meson field self-interaction terms. We find the two models yield, at lower densities, similar results for the bulk static properties of nuclear matter. However, at increasing baryon density, the predictions of the models start to deviate significantly from each other, as for instance in the predictions for the maximum mass of a neutron star or in the role of hyperon degrees of freedom in dense matter. The results also indicate that, with increasing density, scalar meson self-couplings beyond the fourth order seem to play a significant role.

As the final topic of this overview, we consider in the following neutron stars as potential sources of gravitational waves (GWs).

4 GW Emission from Phase Transitions in Neutron Stars

The first generation of large gravitational interferometric detectors as the French-Italian VIRGO and the American LIGO, should be fully operational within one or two years. The best signal-to-noise (S/N) ratio that can be achieved from these detectors implies the use of matched-filter techniques, that require a priori the knowledge of the signal waveform. Thus, the identification of possible sources for gravitational waves having a well defined signal is a relevant problem in the detection strategy.

Neutron stars are certainly one of the most popular potential sources of gravitational waves (GWs), since they can emit by different mechanisms. Here we concentrate our discussion to non-radial oscillations, a mechanism which was discussed in the late sixties[22]. One of the difficulties with this mechanism concerns the energy source necessary to excite the oscillations. The elastic energy stored in the crust and released by tectonic activity was recently considered[23], but the maximum available energy is likely to be of the order of 10^{44-45} erg. Thus, even if all this energy would be converted into non-radial modes, the maximum distance that a signal could be seen by a laser interferometer like VIRGO is only about 3.0 kpc[23]. This prediction depends, of course, on the adopted EoS, which fixes the mode frequencies and damping time-scales. A considerable amount of energy would be available if the neutron star undergoes a phase transition in the core. For instance, if quark deconfinement occurs, then the star will suffer a micro-collapse, since the EoS of quark matter is softer than that of hadronic matter and the new equilibrium configuration will be more compact, having a larger binding energy. The energy difference, reduced by the energy absorption of the phase transition, is partially used to excite mechanical modes, which have energy dissipated by different channels. The structural rearrangement suffered by a "cold" star occurs on a dynamical timescale of the order of milliseconds[24], which is much shorter than the gradual transition expected to occur in hot protoneutron stars[25]. Radial modes excited by the micro-collapse do not radiate GWs, but an important coupling with rotation exists[26] and, if the star rotates, the oscillations will be damped not only by dissipation of the mechanical energy into heat but also by the emission of GWs.

In a recent work[27], the detectability of GWs generated by oscillations excited during a phase transition in the core of a neutron star is reviewed. Neutron star properties were computed using a description of the hadronic matter based on the work of J. Boguta and A.R. Bodmer[5], including the fundamental baryon octet, the isovector meson ϱ and lepton degrees of freedom (see Ref.[27] for details). Hybrid models, including a quark-gluon core, with the *same baryonic number* as the pure hadron configuration were also computed using the MIT bag model. The maximum energy available to excite mechanical oscillations in the star or to be converted into heat was estimated as the energy difference of both configurations, with and without a quark-gluon core. Then, using the planned sensitivity of present laser interferometers like VIRGO (or LIGO I) and those of the next generation (LIGO II), the maximum volume of space that can be probed by these experiments was calculated, as an indication for the potential detectability of these sources of GWs.

Inspection on Table 7, where we show some of the results of our

ν_0 (kHz)	P_{crit} (ms)	τ_{gw} (ms)	Q -	D_{max} ($VIRGO$)	D_{max} ($LIGOII$)
1.62	1.64	87.0	442	4.9	10.2
1.83	1.25	27.0	155	6.4	13.5
2.06	1.13	17.0	110	6.0	12.8
2.32	1.06	11.5	84	5.1	11.1
2.72	1.00	8.4	72	3.6	5.7

Table 7. Oscillation parameters: the damping timescale τ_{gw} is given for the critical period; maximum distances for VIRGO (V) and LIGO II (L) are in Mpc.

calculations[27], indicates that the maximum distance probed by detectors of first generation (VIRGO, LIGO I) is about 6.4 Mpc, well beyond M31, whereas the second generation (LIGO II) will probably see phase transition events at distances two times larger, but certainly not yet attaining the Virgo cluster. The small probed volume and the rapid rotation required for this mechanism to be efficient result in a low event rate, imposing severe limitations on the detectability of such a signal[27].

Concluding Remarks

The topics we have considered in this overview represent just first attempts towards a more profound comprehension on the physical properties of neutron stars. Our main findings are substantiated by a few phenomenological results. However, more involved calculations based on improved microscopic models are needed to strengthen our present knowledge on these topics, which should include, as an example, in the spirit of the Brown-Rho scaling, a density dependence of the coupling constants in the models, rotation and the presence of strong magnetic fields[28]. Investigations along these and other lines are presently in progress.

Acknowledgements

César A. Zen Vasconcellos acknowledges the *Coordenação de Aperfeiçoamento de Pessoal de Nível Superior (CAPES)*, Brazil and the *Instituto de Cibernética, Matemática y Física (ICIMAF)*, Cuba, for financial support for his participation on the it International Workshop on Strong Magnetic Fields and Neutron Stars.

References

1. A. Hewish, S. J. Bell, J. D. H. Pikington, P. F. Scott and R. A. Collins, *Nature* **217**, 709 (1968).
2. N. K. Glendenning, *in Compact Stars* (Springer-Verlag, Berlin, 1997).
3. O. Barziv, L. Kaper, M.H. van Kerkwijk, J.H. Telting, J. van Paradijs, astro-ph/0108237.
4. J. D. Walecka and B. D. Serot, *in Advances in Nuclear Physics* **16** (Plenum Press, New York, 1986).
5. J. Boguta and A. R. Bodmer, *Nucl. Phys.* **A292**, 413 (1977).
6. A.R. Taurines, Master of Sciences Thesis, PhD Thesis, UFRGS, Porto Alegre, Brazil, (1999, http//www.if.ufrgs.br/hadrons/Thesis.html).
7. A. R. Taurines, C. A. Z. Vasconcellos, M. Malheiro and M. Chiapparini, *Phys. Rev.* **C63**, 1 (2001); *Modern Phys. Lett.* **A15**, 1789 (2000).
8. S. S. Rocha, A. R. Taurines, C. A. Z. Vasconcellos, M. Dillig and M. B. Pinto, *Modern Phys. Lett.* **A17**, 1335 (2002).
9. W. Koepf, M. M. Sharma, and P. Ring, Nucl. Phys. **A533**, 95 (1992).
10. N. K. Glendenning, F. Weber, S. A. Moszkowski, *Phys. Rev.* **C45**, 844 (1992).
11. J. Zimanyi, S. A. Moszkowski, *Phys. Rev.* **C42**, 1416 (1990).
12. R. C. Tolman, *Phys. Rev.* **55**, 364 (1939).
13. J. R. Oppenheimer and G. M. Volkoff, *Phys. Rev.* **55**, 374 (1939).
14. G.F. Marranghello, Master of Sciences Thesis, PhD Thesis, UFRGS, Porto Alegre, Brazil, (2000, http//www.if.ufrgs.br/hadrons/Thesis.html).
15. G.F. Marranghello, C.A.Z. Vasconcellos, M. Dillig, J.A. de Freitas Pacheco, *Int. Journ. of Mod. Phys.* **E11**, 83 (2002).
16. M. Prakash, I. Bombaci, M. Prakash, P.J. Ellis, J.M. Lattimer, J.M. and R. Korren, *Phys. Rep.* **280**, 1 (1997).
17. A. Chodos, R.L. Jaffe, K. Johnson, C.B. Thorn and V.F. Weisskopf, *Phys. Rev.* **D9**, 3471, (1974).
18. L. Landau and E. Lifchitz, *in Mécanique Statistique* (Éditions Mir,Moscow, 1967).
19. S.A. Chin, *Ann. Phys.* **108**, 301 (1977).
20. E.K. Heide and S. Rudaz, *Phys. Lett.* **B262**, 375 (1991).
21. M. Prakash, P.J. Ellis, E.K. Heide, S. Rudaz *Nucl. Phys.* **A575**, 583 (1994).
22. K.S. Thorne, A. Campolattaro, *ApJ* **149**, 591 (1967).
23. J.A. de Freitas Pacheco, *A&A* **336**, 397 (1998).
24. P. Haensel, M. Prózynski, *ApJ* **258**, 306 (1982).
25. T.W. Baumgarte, H.-T. Janka, W. Keil, S.L. Shapiro, S.A. Teukolsky, *ApJ* **468**, 823 (1996).
26. W.-Y. Chau, *ApJ* **147**, 664 (1967).
27. G.F. Marranghello, C.A.Z. Vasconcellos and J.A. de Freitas Pacheco, *Phys. Rev* , **D66**, 1 (2002).
28. E. Rodriguez Querts, A. Martin Cruz, H. Perez Rojas, *Int. J. Mod. Phys.* **A17**, 561 (2002).